Eur Biophys J (2005) 34: 1030–1040
DOI 10.1007/s00249-005-0488-6

ARTICLE

M. A. Kiselev · N. Y. Ryabova · A. M. Balagurov
S. Dante · T. Hauss · J. Zbytovska · S. Wartewig
R. H. H. Neubert

New insights into the structure and hydration of a stratum corneum lipid model membrane by neutron diffraction

Received: 24 December 2004 / Revised: 3 March 2005 / Accepted: 26 April 2005 / Published online: 20 July 2005

Abstract The structure and hydration of a stratum corneum (SC) lipid model membrane composed of *N*-(α-hydroxyoctadecanoyl)-phytosphingosine (CER6)/cholesterol (Ch)/palmitic acid (PA)/cholesterol sulfate (ChS) were characterized by neutron diffraction. The neutron scattering length density across the SC lipid model membrane was calculated from measured diffraction peak intensities. The internal membrane structure and water distribution function across the bilayer were determined. The low hydration of the intermembrane space is a major feature of the SC lipid model membrane. The thickness of the water layer in the SC lipid model membrane is about 1 Å at full hydration. For the composition 55% CER6/25% Ch/15% PA/5% ChS, in a partly dehydrated state (60% humidity) and at 32°C, the lamellar repeat distance and the membrane thickness have the same value of 45.6 Å . The hydrophobic region of the membrane has a thickness of 31.2 Å . A decrease of the Ch content increases the membrane thickness. The water diffusion through the SC lipid model multilamellar membrane is a considerably slow process relative to that through phospholipid membranes. In excess water, the membrane hydration follows an exponential law with two characteristic times of 93 and 44 min. At 81°C and 97% humidity, the membrane separates into two phases with repeat distances of 45.8 and 40.5 Å . Possible conformations of CER6 molecules in the dry and hydrated multilayers are discussed.

Keywords Ceramide · Stratum corneum · Lipid membrane · Neutron diffraction

Abbreviations CER1 30-Linoyloxytriacontanoic acid-[(2*S*,3*R*)-1,3-dihydroxyocta-dec-4-en-zyl]-amide · CER6 *N*-(α-Hydroxyoctadecanoyl)-phytosphingosine · Ch Cholesterol · ChS Cholesterol sulfate · DMPC Dimyristoylphosphatidylcholine · DPPC Dipalmitoylphosphatidylcholine · FWHH Full width at half height · HH Hydrophobic–hydrophilic · PA Palmitic acid

M. A. Kiselev · J. Zbytovska · R. H. H. Neubert
Institute of Pharmaceutical Technology and Biopharmacy,
Martin Luther University, Halle, Saale, Germany

M. A. Kiselev (✉) · N. Y. Ryabova · A. M. Balagurov
Frank Laboratory of Neutron Physics,
Joint Institute for Nuclear Research,
Dubna, 141980 Moscow Region, Russia
E-mail: kiselev@jinr.ru
Tel.: +7-096-2166977
Fax: +7-096-2165484

S. Wartewig
Institute of Applied Dermatopharmacy,
Martin Luther University, Halle, Saale, Germany

S. Dante · T. Hauss
Hahn-Meitner Institute, Berlin, Germany

Introduction

The stratum corneum (SC), the outermost layer of the mammalian skin, exhibits the major skin barrier (Wertz and Bergh 1998). To know the structure and properties of the SC on the molecular level is essential for studying drug penetration through the SC and the design of new dermal drug delivery systems. The SC consists of corneocytes embedded in a lipid matrix through which water penetrates. In this respect, an important subject is the structure of the SC lipid matrix and water diffusion through it (Bouwstra et al. 2003).

X-ray and neutron scattering are effective methods in order to characterize the SC, the SC lipid matrix and SC lipid model membranes. It was shown by small-angle X-ray diffraction that the lipid part of the SC forms a lamellar liquid crystal (Friberg and Osborne 1985). The lipid matrix of the SC exhibits a periodicity of 130 Å as shown by X-ray diffraction (White et al. 1988). Small-angle neutron scattering experiments on the SC have provided information which supports the "brick and mortar model" (Charalambopoulou et al. 2000).

Information about the internal structure of SC isolated from skin epidermis is difficult to obtain from diffraction experiments. So far, only the first-order diffraction peak could be detected from such SC membranes. Small-angle and wide-angle diffraction were used to characterize how octyl glucoside influences the structure of pig SC (Lopez et al. 2000). For porcine SC, periodicities of 57 Å (dry state) and 62.8 Å (fully hydrated state) were determined from neutron diffraction (Charalambopoulou et al. 2002).

More information about the structure of SC lipid membranes was obtained using samples prepared from isolated or synthetic ceramides. The SC lipids isolated from mammalian skin form two lamellar phases with periodicities of 64 and 130 Å as measured by X-ray diffraction. A "sandwich model" of the SC matrix was proposed on the basis of these two periodicities (Bouwstra et al. 2001). The presence of 30-linoyloxytriacontanoic acid-[(2*S*,3*R*)-1,3-dihydroxyocta-dec-4-enzyl]-amide (CER1) is crucial for the formation of the 130 Å periodicity. Transmission electron microscopy and X-ray diffraction experiments have confirmed the "sandwich model" (Hill and Wertz 2003; McIntosh 2003).

Since SC lipids play an important role in the skin barrier function for water, it is of great importance to elucidate the effect of hydration on the organization of SC lipids. X-ray diffraction studies revealed that SC lamellae do not swell with increasing content of water (Bouwstra et al. 2003). However, it was shown by neutron diffraction of the SC separated from porcine skin that the membrane swells under full hydration and that the degree of hydration influences the lamellar order (Charalambopoulou et al. 2002).

Nowadays, there is a general consensus that nine types of ceramides determine the major properties of the SC lipid matrix (Jager et al. 2004). There are two approaches to mimicking the SC lipid matrix. One is based on ceramides isolated from mammalian skin and the other one on synthetic ceramides (Friberg and Osborne 1985; Jager et al. 2004).

Calculation of the scattering length density profile based on X-ray or neutron diffraction experiments is a prospective method for investigating the internal structure of the SC lipid matrix. Finding the sign of the structure factor is the crucial limitation for the application of X-ray diffraction (McIntosh 2003). Neutron diffraction overcomes this limitation because the sign of the structure factor can be decided by substituting D_2O for H_2O (Worcester 1976).

An oriented multilamellar stack of phospholipids on a quartz slide is commonly used to reach a reasonable structural resolution in neutron diffraction experiments (Worcester 1976; King and White 1986; Wiener and White 1991; Gordeliy and Kiselev 1995).

The objective of the present article is to characterize the internal structure and hydration of SC lipid model membranes composed of *N*-(α-hydroxyoctadecanoyl)phytosphingosine (CER6)/cholesterol (Ch)/palmitic acid (PA)/cholesterol sulfate (ChS) and deposited on a quartz slide by using neutron diffraction. The composition ratio CER6/Ch/PA/ChS was similar to that used by Wertz et al. (1986) and Hatfield and Fung (1995).

Materials and methods

Materials

The CER6 (Fig. 1) was a gift from Cosmoferm (Delft, The Netherlands). Dimyristoylphosphatidylcholine (DMPC) was offered by Lipoid (Ludwigshafen, Germany). Ch, ChS and PA were purchased from Sigma-Aldrich (Taufkirchen, Germany). Quartz slides (Spectrosil 2000) were obtained from Saint-Gobain (Germany).

Sample preparation

Three compositions of the quaternary system CER6/Ch/PA/ChS were studied, namely the component ratios 66/10/18/6, 55/25/15/5 and 44/40/12/4 (w/w), where the weight ratio CER6/PA/ChS was kept as 11/3/1.

The multilayer lipid films were deposited from organic solution on a quartz slide according to the procedure of Seul and Sammon (1990). The appropriate mixture of lipids was dissolved in chloroform/methanol (1/1 w/w) at a concentration of 10 mg/ml. A volume of 600 µl of the solution was spread over a 3.2 cm×2.5 cm quartz surface and dried at room temperature. The rest of the organic solvent was removed under vacuum. The sample was heated in a horizontal position above 80°C to decrease the sample mosaicity. The thickness of the lipid film on the quartz slide was $L = 7.5$ µm.

Neutron diffraction experiment

Neutron diffraction patterns from the samples were collected at the V1 diffractometer of the Hahn-Meitner Institute, Berlin, situated at a cold neutron source ($\lambda = 4.517$ AA) with a sample-to-detector distance of 101.8 cm. Diffraction patterns were recorded as sample rocking curves at several fixed scattering angles 2Θ of the two-dimensional position sensitive ^{3}He detector

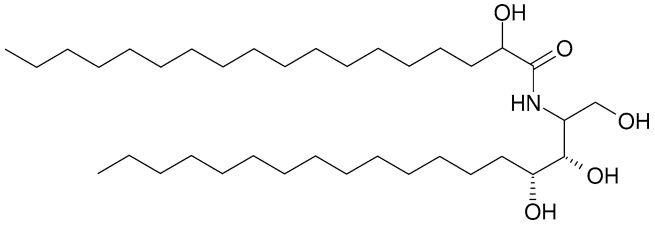

Fig. 1 Chemical structure of the *N*-(α-hydroxyoctadecanoyl)-phytosphingosine (*CER6*) molecule

(20 cm×20 cm area, 1.5 mm×1.5 mm spatial resolution). Samples were studied at temperatures of 32 and 82°C at humidities of 60 and 99% as well as in excess water. Samples were equilibrated for 12 h in a chamber at fixed humidity and temperature prior to the measurements.

Resolution of the Fourier synthesis

A reasonable model for the internal bilayer structure depends on the space resolution Δx of the Fourier synthesis. Roughly speaking, the location of molecular groups in a bilayer model can be resolved if the groups are separated by a distance Δx. Therefore, it is important to consider the origin of the resolution in detail.

For the one-dimensional and even scattering length density $\rho(x)$ of the bilayer unit in the multilamellar membrane, the distribution of the structure factor $F(q)$ in reciprocal space is connected to $\rho(x)$ by Fourier transformation (Feigin and Svergun 1987):

$$\rho(x) = \frac{1}{4\pi}\int_0^\infty F(q)\,\cos(qx)\,\mathrm{d}q. \tag{1}$$

The limitation in the space resolution Δx is associated with the possibility to measure h_m diffraction peaks. A diffraction peak of the order of h_m is located at $q_\mathrm{m} = 2\pi h_\mathrm{m}/d$ in the reciprocal space; d is the lamellar repeat distance. The measured distribution $F_\mathrm{exp}(q)$ can be described by

$$F_\mathrm{exp}(q) = F(q)\,\varphi(q), \tag{2}$$

where $F(q)$ is determined in the range $0 \le q < \infty$. The step function $\phi(x)$ is given by $\phi(x) = 1$ if $0 \le q \le q_\mathrm{max}$ and $\phi(x) = 0$ if $q > q_\mathrm{max}$. According to the properties of the Fourier transformation, the experimentally determined $\rho_\mathrm{exp}(x)$ can be presented as convolution

$$\rho_\mathrm{exp}(x) = \int_0^\infty \rho(y)\,\rho_0(x-y)\,\mathrm{d}y, \tag{3}$$

where $\rho(x)$ is the true scattering length density of the lipid membrane and $\rho_0(x)$ is the Fourier transform of $\phi(q)$:

$$\rho_0(x) = \frac{1}{4\pi}\int_0^{q_\mathrm{m}} \cos(qx)\,\mathrm{d}q = \frac{q_\mathrm{m}}{4\pi}\,\frac{\sin(q_\mathrm{m}x)}{(q_\mathrm{m}x)}. \tag{4}$$

Considering Eq. 3, any peak in the scattering length density $\rho(x) = \delta(x)$ is smeared and the experimentally determined scattering length density is given by

$$\rho_\mathrm{exp}(x) \sim \frac{\sin(\mathrm{q_m}x)}{\mathrm{q_m}x}. \tag{5}$$

Figure 2 presents Eq. 5 for two peaks located at $q_\mathrm{m}x = 0$ and π. The function in Eq. 5 is zero at $x_1 = \Delta x_1 = (\pi/q_\mathrm{m}) = (d/2h_\mathrm{m})$ and at $x_2 = \Delta x_2 = (2\pi/q_\mathrm{m}) = (d/h_\mathrm{m})$. The resolution Δx_2 corresponds to the full peak separation (Wiener and White 1991; Hristova and White 1998). The resolution Δx_1 corresponds to the peak overlapping as presented in Fig. 2 (King and White 1986; Gordeliy and Kiselev 1995). The two δ functions $\rho_1(x) = \delta(q_\mathrm{m}x)$ and $\rho_2(x) = \delta(q_\mathrm{m}\ x-\pi)$, shifted to each other by the distance $\Delta x_2 = d/h_\mathrm{m}$, are smeared to the functions presented in Fig. 2. This smeared functions cross each other at the point above the half height of the peaks. We consider two peaks to be resolved experimentally in the case of the crossing point at the full width at half height (FWHH). The FWHH of the function $\rho_\mathrm{exp}(x)$ is given by

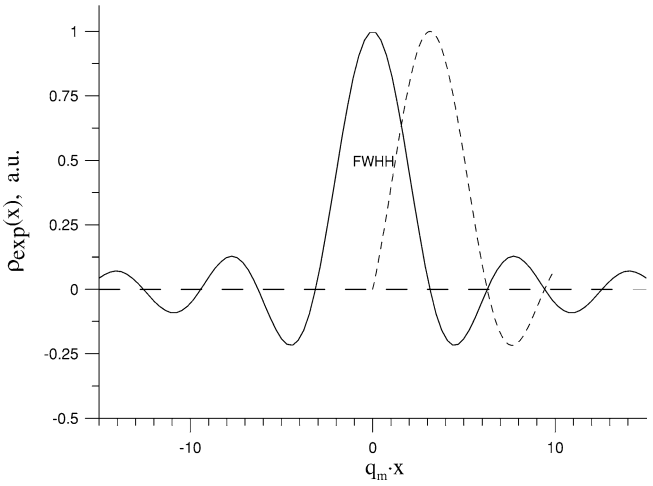

Fig. 2 Experimentally determined scattering length density $\rho_\mathrm{exp}(x)$ from the true scattering density $\rho_1(x) = \delta(q_\mathrm{m}\ x)$ and $\rho_2(x) = \delta(q_\mathrm{m}\ x-\pi)$, *solid line* and *dashed line*, respectively. Only a part of $\rho_\mathrm{exp}(x)$ is presented for $\rho_2(x)$

$$\mathrm{FWHH} = \frac{3.8}{q_\mathrm{m}} = \frac{3.8\,d}{2\pi\,h_m} \approx 0.6\,\frac{d}{h_\mathrm{m}}. \tag{6}$$

This value of the FWHH is used as the resolution for our diffraction experiment.

Results

Structure of membranes at equilibrium conditions

The measured rocking curves for the composition 55/25/15/5 are presented in Fig. 3 for the case of 60% humidity, 8% D_2O and 32°C. The low mosaicity of the sample (0.12°) allows one to collect five orders of neutron diffraction. The membrane repeat distance $d = 45.68 \pm 0.05$ Å was calculated from the peak positions. The space resolution achieved amounts to $0.6(d/h_\mathrm{m}) = 5.5$ Å, where $h_\mathrm{m} = 5$ is the maximum diffraction order. This space resolution allows one to apply the model of the internal membrane structure as hydrophobic and hydrophilic parts and to

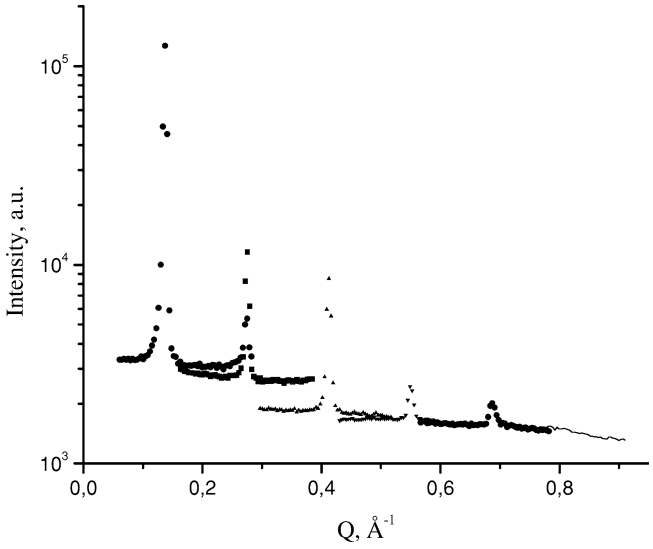

Fig. 3 Rocking curves measured at six different detector angles (7, 11.2, 16.8, 22.4, 28, 33.6°) for the CER6/cholesterol (*Ch*)/palmitic acid (*PA*)/cholesterol sulfate (*ChS*) membrane with the composition 55/25/15/5 at 60% humidity, 8% D_2O and 32°C

introduce molecular groups separated in distances of about 6 Å .

The linear absorption coefficient for the composition 55/25/15/5 in the dry state was calculated as $\mu = 6.1\ \mathrm{cm}^{-1}$, which is near the absorption of a CH_2 chain, $\mu = 6.0\ \mathrm{cm}^{-1}$, and is a little bit larger than the absorption of dry DMPC, $\mu = 5.5\ \mathrm{cm}^{-1}$. The absorption coefficients for the structure factor correction of dry composition 55/25/15/5 are calculated as (Franks and Lieb 1979)

$$A_h(\Theta) = \left\{ \frac{\sin\Theta}{2\,\mu L}\left[1 - \exp\left(-\frac{2\,\mu L}{\sin\Theta}\right)\right]\right\}^{-1/2} \qquad (7)$$

and are 1.05, 1.02, 1.02, 1.01, 1.01 and 1.01 for diffraction orders $h = 1$, 2, 3, 4, 5 and 6, respectively.

The linear absorption coefficient for H_2O is $\mu = 5.6\ \mathrm{cm}^{-1}$, and that for D_2O is $\mu = 0.6\ \mathrm{cm}^{-1}$. Addition of a 1 Å water layer to the dry lipid bilayer of 45 Å has no influence on the $A_h(\Theta)$. Addition of a 10 Å water layer increases $A_h(\Theta)$ to 1.06, 1,03, 1.02, 1.02, 1.02 and 1.02 for diffraction orders $h = 1$, 2, 3, 4, 5 and 6, respectively. The substitution of H_2O–D_2O shows a 10 times smaller effect. The absorption coefficients are near unity and create not more than 4% deviation in the scattering length density $\rho(x)$. Thus, for the lipid films of 7.5 μm thickness, the consideration of the absorption effects can be omitted.

The absolute values of the structure factors $|F_h| = \sqrt{h\,I_h}$ (h is the diffraction order) were calculated from the integrated peak intensity I_h and were corrected to the Lorentz factor of the oriented membrane (Nagle and Tristram-Nagle 2000). The influence of the absorption on the structure factor values was not taken into account. Isotopic substitution of H_2O–D_2O was used to evaluate the sign of the structure factor (Worcester 1976; Franks 1976; Franks and Lieb 1979). A concentration of 8% (w/w) D_2O in H_2O corresponds to the zero scattering length density of water. The composition 55/25/15/5 was measured at 8, 20 and 50% D_2O concentration at 60% humidity. The calculated repeat distances at various D_2O contents of 45.68 ± 0.05 Å (8% D_2O), 45.62 ± 0.02 Å (20% D_2O) and 45.60 ± 0.06 Å (50% D_2O) show a constant value of d. Thus, the membrane repeat distance averaged over all D_2O concentrations is equal to 45.63 ± 0.04 Å .

The slope of the F_h dependence on the D_2O concentration determines the sign of the structure factor (Franks and Lieb 1979). For the case of a symmetrical membrane with water penetrated into the bilayer, the even-order structure factor increases linearly and the odd-order one decreases linearly with an increase in D_2O content. The calculated values of $|F_h|$ were arranged as a linear function, according to this rule (Fig. 4). The signs of the structure factors were determined from Fig. 4 as −, +, −, +, and − for the diffraction orders $h = 1$, 2, 3, 4 and 5, respectively. The neutron scattering length density (in arbitrary units) across the bilayer $\rho_s(x)$ was restored by Fourier synthesis (Nagle and Tristram-Nagle 2000):

$$\rho_s(x) = \frac{2}{d}\sum_{h=1}^{h_{max}} F_h \cos\left(\frac{2\pi h x}{d}\right). \qquad (8)$$

Fourier profiles for 8, 20 and 50% of D_2O are presented in Fig. 5. The two maxima of the neutron scattering length density correspond to the position of polar head groups of the lipid bilayer, and the minimum of $\rho_s(x)$ at the center of the bilayer corresponds to the position of CH_3 groups of CER6, PA and Ch molecules.

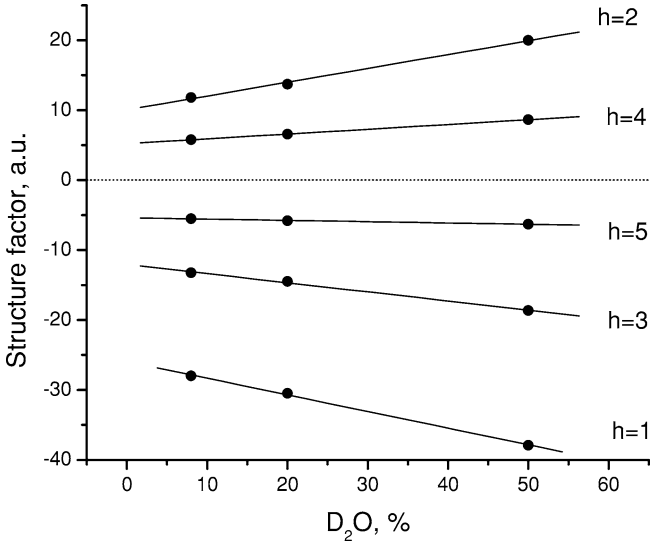

Fig. 4 The dependence of the membrane structure factor F_h of order $h = 1$, 2, 3, 4 and 5 on the D_2O content for the membrane CER6/Ch/PA/ChS with the composition 55/25/15/5: 60% humidity and 32°C

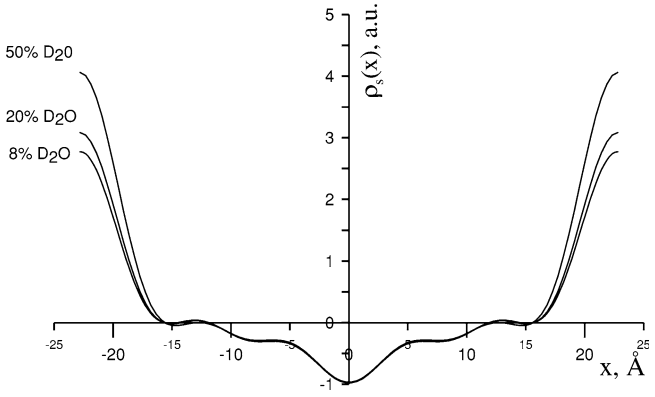

Fig. 5 The neutron scattering length density $\rho_s(x)$ of the CER6/Ch/PA/ChS membrane with the composition 55/25/15/5 at 60% humidity and 32°C for the cases of 8, 20 and 50% D_2O content

The calculated Fourier profile does not show a region of intermembrane space, which is typical for phospholipid membranes (Fig. 6) (Franks and Lieb 1979; Worcester 1976; Gordeliy and Kiselev 1995). The distance between the maxima belonging to polar head groups is $d_{PH} = 45.6$ Å . The same values of d_{PH} and d show that the thickness of the intermembrane space is too small to be resolved in the neutron diffraction experiment. Thus, an important conclusion of the Fourier synthesis is that the membrane thickness is $d_m = d_{PH} = d$ and that the thickness of the water layer is $d_w \approx 0$ at 60% humidity.

To have a comparison with phospholipid membranes, a DMPC multilamellar sample was measured under the same conditions as for the mixed quaternary system. For this membrane six orders of diffraction were collected. The signs of the structure factors −, −, +, −, −, + for the diffraction orders 1, 2, 3, 4, 5 and 6 were taken as described in the literature (Franks and Lieb 1979). The Fourier profile of the DMPC membrane presented in Fig. 6 shows distinct regions of CH_3 and polar head groups, as well as the intermembrane space. The repeat distance is 54.75 ± 0.03 Å and the distance between the maxima belonging to the polar head groups is $d_{PH} = 37.6$ Å .

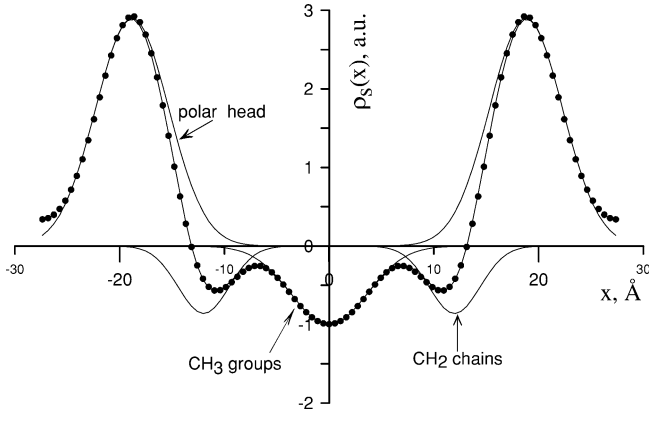

Fig. 6 The neutron scattering length density $\rho_s(x)$ of the dimyristoylphosphatidylcholine membrane at 60% humidity, 32°C, and 8% D_2O content (*dots*) and the fitted curve (*solid line*). *Arrows* mark the three molecular groups: CH_3 groups, CH_2 chains and polar head groups

In the case of the DMPC membrane, a fit of the Fourier profile by Gaussian functions was used to characterize numerically the internal membrane structure. The Fourier profile was fitted by three functions. The function ascribed to methyl group centered at $x = 0$ is given by

$$\rho_{CH_3}(x) = \frac{A}{\sqrt{2\pi}\,\sigma} \exp\left[-\frac{1}{2}\left(\frac{x - x_0}{\sigma}\right)^2\right] \tag{9}$$

with two fit parameters, namely, the area A, and the standard deviation σ. The region of methylene groups and polar head groups was fitted by the function

$$\rho^{sym}(x) = \frac{A}{\sqrt{2\pi}\,\sigma}\left\{\exp\left[-\frac{1}{2}\left(\frac{x - x_0}{\sigma}\right)^2\right] + \exp\left[-\frac{1}{2}\left(\frac{x + x_0}{\sigma}\right)^2\right]\right\}, \tag{10}$$

which described the symmetrical scattering length density distribution relative to $x = 0$. The $\rho^{sym}_{CH_2}(x)$ and $\rho^{sym}_{PH}(x)$ functions have six independent parameters: A, σ and x_0. Finally, the Fourier profile $\rho_s(x)$ was fitted by the function

$$\rho_{fit}(x) = \rho_{CH_3}(x) + \rho^{sym}_{CH_2}(x) + \rho^{sym}_{PH}(x), \tag{11}$$

which comprises eight independent parameters.

The software PeakFit (Systat Software) was used for curve-fitting. The results of fitting are presented in Fig. 6 and Table 1. To characterize the width of the polar head group FWHH $= 2\sigma\sqrt{2\ln 2}$ was used (Gordeliy and Kiselev 1995; Nagle and Tristram-Nagle 2000). The thickness of the DMPC membrane is given by

$$d_m = 2\left(x_0(PH) + \frac{FWHH(PH)}{2}\right) = 45.8 \pm 0.1 \text{ Å}. \tag{12}$$

The thickness of the water layer between the membranes is $d_w = d - d_m = 9.0 \pm 0.1$ Å. The results obtained for the DMPC membrane structure are in agreement with the data derived from X-ray diffraction experiments(Nagle and Tristram-Nagle 2000; Tristram-Nagle et al. 2002).

For the CER6/Ch/PA/ChS membrane four functions were assumed to fit the Fourier profile $\rho_s(x)$:

Table 1 Parameters of the scattering length density profile of the dimyristoylphosphatidylcholine membrane at 60% humidity and 32°C; lamellar repeat distance $d = 54.75 \pm 0.03$ Å

Molecular group	A (a.u.)	x_0 (Å)	σ (Å)	FWHH (Å)[a]
Polar head group	25.25 ± 0.03	18.80 ± 0.05	3.47 ± 0.02	8.17 ± 0.05
CH_2	−5.22 ± 0.05	11.98 ± 0.05	2.43 ± 0.05	5.7 ± 0.1
CH_3	−9.11 ± 0.09	0	3.62 ± 0.02	8.53 ± 0.05

FWHH full width at half height
[a]FWHH $= 2\sigma\sqrt{2\ln 2}$

$$\rho_{\text{fit}}(x) = \rho_{\text{CH}_3}(x) + \rho^{\text{sym}}_{\text{CH}_2}(x) + \rho^{\text{sym}}_{\text{Ch}} + \rho^{\text{sym}}_{\text{PH}}(x). \quad (13)$$

Additionally, $\rho^{\text{sym}}_{\text{Ch}}(x)$ was introduced to determine the position of Ch molecules. The $\rho_{\text{fit}}(x)$ function fits the $\rho_s(x)$ function with good accuracy as seen from Fig. 7.

Table 2 lists the parameters of the molecular groups derived from the diffraction experiment for the composition 55/25/15/5 at 60% humidity and 8% D_2O content. The result deduced from the Fourier profile $\rho_s(x)$ proves that the thickness of the intermembrane water space is nearly zero at 60% humidity. In the case of the DMPC membrane, the Fourier profile exhibits a distinct intermembrane region. The low hydration of the intermembrane space is a major feature of the SC lipid model membrane relative to phospholipids. This peculiarity of the CER6/Ch/PA/ChS membrane can be attributed to the properties of the interface between two leaflets.

Three possible CER6 conformations inside the multilayer are presented in Fig. 8. For the fully extended conformation, the CER6 molecule is symmetrically arranged between two leaflets (Raudenkolb et al. 2005). In this case, the polar group of CER6 is located between two leaflets, and CER6 creates a bridge between the leaflets. Both one-sided and fully extended conformations of CER6 molecules fulfill the requirements of $\rho_s(x)$ presented in Fig. 7.

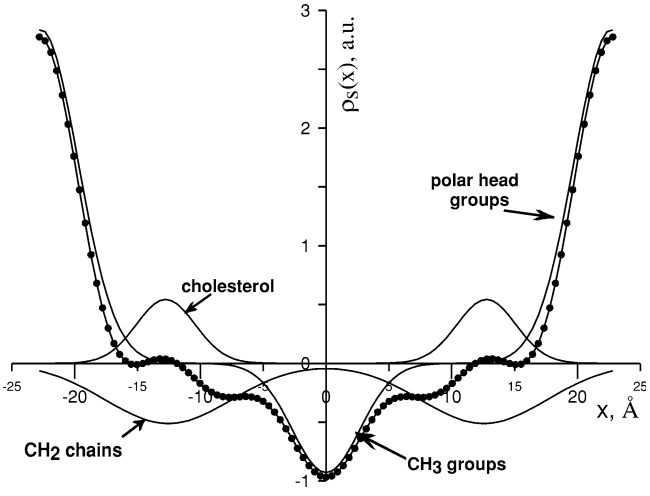

Fig. 7 The neutron scattering length density $\rho_s(x)$ of the CER6/Ch/PA/ChS membrane with composition 55/25/15/5 at 60% humidity, 32°C,and 8% D_2O content (*dots*) and the fitted curve (*solid line*). *Arrows* mark the four components: CH_3 groups, CH_2 chains, cholesterol and polar head groups

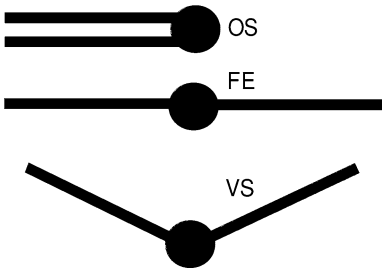

Fig. 8 Three possible conformations of CER6 inside the multilayer: one-sided shape (*OS*), fully extended shape (*FE*) and V shape (*VS*)

In the case of the CER6/Ch/PA/ChS membrane, one Gaussian function fits two polar head groups from neighboring bilayers. Figure 7 presents half of this Gaussian function related to one bilayer. The thickness of the polar head group characterized by FWHH/2 amounts to 3.46 ± 0.01 Å.

A decrease of the Ch content in the membrane increases the membrane repeat distance *d*. At 60% humidity, the repeat distance amounts to 43.9 ± 0.3 Å for the composition 44/40/12/4, 45.63 ± 0.04 Å for the composition 55/25/15/5, and 46.1 ± 0.1 Å for the composition 66/10/18/6. As can be seen from Tables 2 and 3, the decrease in the Ch content from 25 to 10 % increases the width of the polar head group from 3.5 to 3.8 Å and the FWHH of the Ch peak from 5.5 to 6.3 Å. Finally,

Table 3 Parameters of the scattering length density profile of the CER6/Ch/PA/ChS membrane with the composition 66/10/18/6 at 60% humidity and 32°C; lamellar repeat distance $d = 46.1 \pm 0.1$ Å

Molecular group	*A* (a.u.)	x_0 (Å)	σ (Å)	FWHH (Å)[a]
Polar head group	23.4 ± 0.3	23.05[b]	3.23 ± 0.02	7.61 ± 0.05
Cholesterol	3.36 ± 0.84	12.93 ± 0.04	2.66 ± 0.11	6.26 ± 0.26
CH_2	−7.56 ± 0.58	13.83 ± 0.30	4.61 ± 0.39	10.86 ± 0.92
CH_3	−7.17 ± 0.10	0	3.02 ± 0.02	7.11 ± 0.05

[a] FWHH $= 2\sigma\sqrt{2 \ln 2}$
[b] $x_0 = d/2$ is a fixed parameter

Table 2 Parameters of the scattering length density profile of the *N*-(α-hydroxyoctadecanoyl)-phytosphingosine (*CER6*)/cholesterol (*Ch*)/palmitic acid (*PA*)/cholesterol sulfate (*ChS*) membrane with the composition 55/25/15/5 at 60% humidity and 32°C; lamellar repeat distance $d = 45.63 \pm 0.04$ Å

Molecular group	*A* (a.u.)	x_0 (Å)	σ (Å)	FWHH (Å)[a]
Polar head group	20.9 ± 0.09	22.82[b]	2.94 ± 0.009	6.92 ± 0.02
Cholesterol	3.197 ± 0.009	12.760 ± 0.007	2.350 ± 0.007	5.53 ± 0.02
CH_2	−6.437 ± 0.05	12.55 ± 0.03	5.02 ± 0.04	11.82 ± 0.09
CH_3	−6.256 ± 0.09	0	2.690 ± 0.009	6.34 ± 0.02

[a] FWHH $= 2\sigma\sqrt{2 \ln 2}$
[b] $x_0 = d/2$ is a fixed parameter

the Ch peak of the $\rho_s(x)$ function at 10% Ch becomes smaller relative to that at 25% Ch. This experimental fact supports the validity of our model of the lipid bilayer as a combination of four distinct regions: polar head group, Ch, CH_2 chains and CH_3 groups.

The scattering length density $\rho_s(x)$ of the quaternary membrane near the membrane surface increases with increasing D_2O content in the vapor as demonstrated in Fig. 5 for the cases of 8, 20 and 50% D_2O content in the water. This increase occurs in the hydrophilic membrane region and is proportional to the water density distribution function (Kiselev et al. 2004). The water distribution function across the bilayer can be calculated in arbitrary units as difference between $\rho_s(x)$ at 50% D_2O content and 8% D_2O content. The result obtained is presented in Fig. 9. Water penetration into the bilayer proves the validity of the phasing method used. Nevertheless, despite the drastically small hydration of the intermembrane space, the hydration inside the bilayer is similar to that for phospholipids (Nagle and Tristram-Nagle 2000). It allows one to create unilamellar CER6/Ch/PA/ChS vesicles in water (Zemlyanaya et al. 2004).

For the sake of interpretation, one should consider two possible structures of the hydrophobic–hydrophilic (HH) boundary. We determine the hydrophilic region as the region of water penetration inside the bilayer. Thus, the HH boundary is given by the coordinate x where the probability for water molecule location is zero.

In the first approach, the HH boundary is considered as equal to the polar head group boundary with an abrupt decrease in the $\rho_s(x)$ function (Gordeliy and Kiselev 1995; Nagle and Tristram-Nagle 2000; Kucerka et al. 2004). Based on the cutoff model, $X_{HH} = 19.1$ Å is determined as value of x at half maximum of $\rho_w(x)$. The cutoff HH boundary is smoothed after Fourier transformation. Thus, the cutoff HH boundary is not in contradiction to the calculated $\rho_w(x)$.

The second approach (based on computer simulations and small-angle scattering results) takes into account the penetration of water into the hydrocarbon chains (Armen et al. 1998; Kiselev et al. 2004). The water distribution function exhibits a sigmoidal form and is similar to that presented in Fig. 9. The smooth HH boundary gives $X_{HH} = 15.6 \pm 0.1$ Å, as presented in Fig. 9. The 3.5 Å difference between the cutoff and the smooth HH boundary is within the accuracy of Fourier synthesis (5.5 Å). To improve the accuracy, additional independent experimental information is needed. The value $X_{HH} = 15.6 \pm 0.1$ Å is supported by the value $X_{HH} = 14.5 \pm 2$ Å calculated from a small-angle scattering experiment on unilamellar vesicles from CER6/Ch/PA/ChS with the composition 55/20/15/10 (Zemlyanaya et al. 2004).

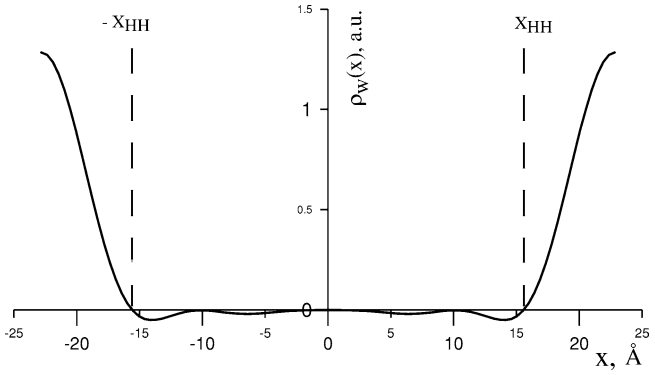

Fig. 9 Water distribution function $\rho_w(x)$ across the CER6/Ch/PA/ChS membrane with the composition 55/25/15/5 at 32°C and 60% humidity. The hydrophobic–hydrophilic boundary (*HH*) is denoted by *dashed lines*. $X_{HH} = 15.6 \pm 0.1$ Å

With increasing hydration of the 55/25/15/5 composition from 60 to 99% humidity at 32°C, the repeat distance d increases from 45.63 ± 0.04 to 46.13 ± 0.1 Å. These values of d were measured after equilibration at fixed temperature and humidity. The equilibrium value of d in excess water is 46.45 ± 0.03 Å . The number of diffraction peaks decreases from 5 to 3 after depositing the sample in the chamber with excess water, and a Fourier analysis based on three diffraction peaks is not useful.

The structural results obtained for the CER6/Ch/PA/ChS membrane at equilibrium conditions are summarized in Table 4. It is not possible to determine the thickness of the water layer d_w in terms of the Fourier synthesis with the resolution of 5.5 Å . Therefore, $d_w = 0.82 \pm 0.07$ Å was calculated as the difference between the membrane repeat distances in excess water and at 60% humidity.

The pattern from the composition 55/25/15/5 at 81°C and 97% humidity shows only three diffraction peaks split owing to the two phases: one phase with $d = 45.84 \pm 0.17$ Å, which is near to the repeat distance at 32°C, and the other phase with a decreased value of $d = 40.52 \pm 0.04$ Å.

Kinetics of the membrane hydration

The kinetics of hydration of the SC lipid model membrane was measured by a time-resolved diffraction technique at 25°C. A dry sample with the composition

Table 4 Structural parameters of the CER6/Ch/PA/ChS membrane with the composition 55/25/15/5 at full hydration and 32°C

Repeat distance at full hydration (Å)	Membrane thickness (Å)	Thickness of water layer (Å)	Thickness of hydrophilic region (Å)	Thickness of hydrophobic core (Å)
46.45 ± 0.03	45.63 ± 0.04	0.82 ± 0.07	7.22 ± 0.24	31.2 ± 0.2

55/25/15/5 was introduced into the chamber with excess water (50% D_2O). The first-order diffraction peak was collected for 1 h with an acquisition time of 1 min and time intervals of 6 min between measurements. Then, the acquisition time was increased to 10 min and the time interval between measurements was increased to 1 and 6 h.

The exponential increase of the membrane repeat distance due to hydration is demonstrated in Fig. 10. During the full hydration, the repeat membrane distance increases by $\Delta d_0 = 1.18 \pm 0.05$ Å from 45.3 ± 0.5 Å for the dry state (room humidity 30–40%). The value of the membrane thickness in the dry state, 45.3 ± 0.5 Å, has a large error in comparison with that from with the static experiment. In the static experiment, the value of q was calibrated to the zero-scattering angle. This calibration requires the acquisition of at least two diffraction peaks. Only one peak was collected during the first hour in the kinetics experiment. Nevertheless, the relative change in the repeat distance Δd was calculated with good accuracy. The membrane swelling due to hydration can be described by

$$\Delta d = \Delta d_0 \left[1 - \exp\left(-\frac{t}{\tau}\right)\right] \tag{14}$$

with a characteristic time of 93 ± 6 min. Assuming a constant membrane thickness, it is possible to derive the thickness of the water layer as $d_w = 1.18$ Å from the kinetics experiment.

Membrane swelling can be caused by changes in the intermembrane water layer or changes in the thickness of the membrane. According to Eq. 8, changes in the structure factor F_h reflect appropriate changes in $\rho_s(x)$, which is connected with molecular group arrangements in the lipid bilayer. Figure 11 presents the time dependence of the absolute value of the first-order structure factor F_1 during the hydration. At the beginning of hydration, the F_1 value increases exponentially according to Eq. 14 with a characteristic time of 44 min. After 1 h of hydration, there is a drastic change in the value of F_1, which reflects changes in the internal membrane structure.

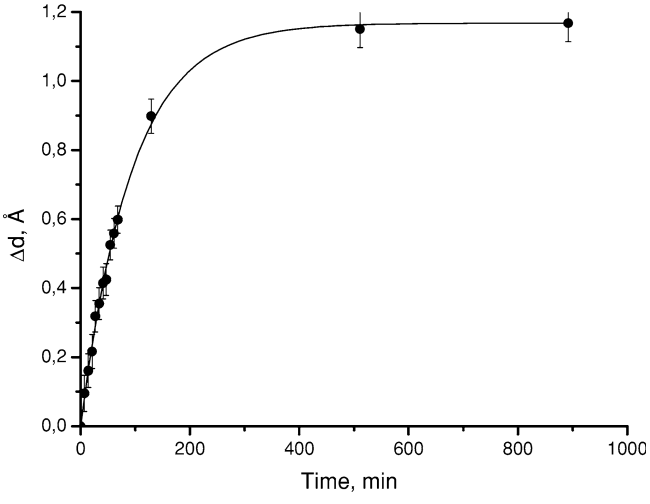

Fig. 10 Kinetics of membrane swelling Δd in excess water at 25°C for the CER6/Ch/PA/ChS membrane with the composition 55/25/15/5. Experimental points and the fitted exponential curve are described with a characteristic time of 93 ± 6 min

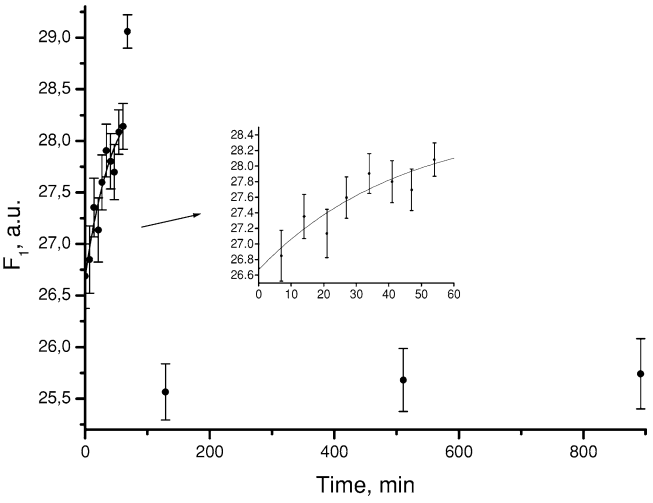

Fig. 11 Kinetics of the membrane first-order structure factor due to swelling in water. The CER6/Ch/PA/ChS membrane with composition 55/25/15/5 at 25°C

Discussion

The structural changes of the gel phase of DMPC due to full hydration from a partly dry state are as follows: the repeat distance d increases by 4.3 Å from 55.6 to 59.9 Å, the membrane thickness d_m decreases by 0.1 Å from 48.3 to 48.2 Å, and the thickness of the water layer d_w increases by 4.4 Å from 7.3 to 11.7 Å (Tristram-Nagle et al. 2002). For a one-component lipid membrane, the membrane thickness depends on the hydration as follows:

$$d_m = \frac{V + n_w V_w}{A}, \tag{15}$$

where V is the volume of dry lipid molecules, A is the surface area per DMPC molecule, V_w is the volume of a water molecule, and n_w is the number of water molecules located in the hydrophilic region of one lipid molecule. According to Eq. 15, the membrane thickness d_m under hydration can decrease owing to the penetration of water molecules into the polar head groups and/or owing to an increase of A or it can be constant if n_w is constant and A is constant. One should consider membrane thickness as constant under hydration from partly dehydrated membranes. This finding supports our assumption of a constant membrane thickness under hydration of the SC lipid model membrane from 60% humidity or 30–40% (room humidity) to the fully hydrated system. The values obtained for the thickness of the water layer d_w are 0.82 ± 0.07 Å at full hydration from 60% humidity and 1.18 ± 0.05 Å at full hydration

from room humidity. One can calculate the thickness of the water layer in the CER6/Ch/PA/ChS membranes as 1.0 ± 0.1 Å from both experimental values. This value is about 10 times smaller than the thickness of the water layer for phospholipid membranes in the gel phase: DMPC—11.7 Å, dipalmitoylphosphatidylcholine (DPPC)—11.1 Å (Tristram-Nagle et al. 2002; Nagle and Tristram-Nagle 2000).

At 25 and 10% Ch, the thicknesses of polar head groups amount to 3.5 and 3.8 Å, respectively, which are smaller than the 8.2 Å thickness of polar head groups of the DMPC membrane and reflect the small polar groups of ceramide, PA and Ch molecules.

Water molecules penetrate 3.8 Å deep into the region of hydrocarbon chains similar as for a phospholipid membrane (Armen et al. 1998; Kiselev et al. 2004). The thickness of the hydrophobic core of the membrane is 31.2 ± 0.2 Å .

The location of the Ch peak at 12.8 Å corresponds to the position of the steroid nuclei. The neutron scattering length of hydrogen is negative. The region of the steroid nuclei exhibits a minimum density of hydrogen that corresponds to a maximum in the scattering length density profile. The location of Ch in the SC model lipid membrane looks similar to the location of Ch in phospholipid membranes (Franks and Lieb 1979). The exact position of Ch could not be determined owing to the limited resolution of the experiment. Probably, the maximum of the Ch peak corresponds to the boundary between A and B steroid nuclei. Further progress in the determination of the Ch position in the SC lipid model membrane could be achieved by applying partly deuterated Ch.

On the basis of the neutron diffraction data, we propose the structural model presented in Fig. 12 for the CER6/Ch/PA/ChS membrane with the composition 55/25/15/5 in excess water at 32°C.

The low hydration of the intermembrane space of the SC lipid model membrane is an essential distinction from a phospholipid membrane. A concentration of Ch above 0.03–0.04 mol increases the membrane bending rigidity and decreases the membrane undulation (Lemmich et al. 1996). A decreased undulation force between membranes and the small value of hydration can be a reason for the remarkably small thickness of the water layer between the membranes (Rand and Parsegian 1989).

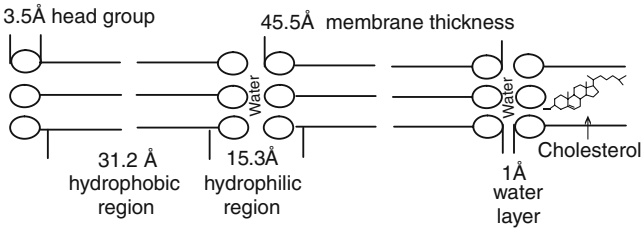

Fig. 12 Schematic representation of the CER6/Ch/PA/ChS membrane with the composition 55/25/15/5 at full hydration and 32°C

The thickness of the intermembrane space is almost zero at 60% humidity. The polar groups of lipid molecules from opposite bilayers create the interface between two membrane leaflets. This effect of "polar group adhesion" has a fundamental consequence for the "sandwich model" of the SC lipid matrix. The sandwich model of the SC lipid matrix was suggested in order to elucidate the X-ray scattering and electron transmission data on lipid membrane from epidermal SC (Bouwstra et al. 2001; Hill and Wertz 2003). In this model, the SC membrane consists of 130 Å trilamellar repeat units with internal layers of 50, 30 and 50 Å. Our finding shows that an arrangement is possible without internal layers of water inside the 130 Å trilamellar repeat unit. Moreover, the absence of a water layer between the 30 and 50 Å subunits creates the best conditions for the penetration of CER1 from the 50 Å layer to the 30 Å layer.

CER6 consists of the diastereomeric forms D-CER6 and L-CER6 (Raudenkolb et al. 2005) . In the crystalline phase L-CER6 forms a V-shaped structure with a spacing of 36 Å (Fig. 8). This conformation of L-CER6 does not match the 45.6 Å spacing of the CER6/Ch/PA/ChS membrane at 60% humidity. In the CER6/Ch/PA/ChS membrane, probably, the one-sided conformation of L-CER6 is energetically preferred. The fully extended spacing of crystalline D-CER6 of 44 Å is in agreement with the repeat distance of the CER6/Ch/PA/ChS membrane. We suppose that D-CER6 molecules or some of them appear in the fully extended conformation in the CER6/Ch/PA/ChS membrane at 60% humidity. The fully extended form of D-CER6 is energetically preferred in the completely dry CER6/Ch/PA/ChS membrane.

The second important feature of the CER6/Ch/PA/ChS membrane is the long duration of the water diffusion through the membrane from a surrounding medium. The investigation of water diffusion through a mutilamellar oriented DPPC membrane hydrated from room humidity to 99% shows an exponential increase of the first-order structure factor with a characteristic time of 9 min (Balagurov et al. 1986). In the case of mutilamellar DPPC vesicles in excess water, the free water diffusion from fully hydrated DPPC to the bulk solvent is completed in 1 min under freeze-induced dehydration (Kiselev et al. 2000).

The increase of the first-order structure factor and of the repeat distance during hydration of the SC lipid model membrane reveals characteristic times of 44 and 93 min, respectively. This big difference relative to DPPC reflects the slow water diffusion through the SC lipid model membranes. The fully extended conformation of D-CER6 in the multilamellar membrane can be a reason for the slow water diffusion.

The kinetics of water diffusion through SC lipid model membranes consists of two parts: hydration of the intermembrane space and hydration of the hydrophilic membrane region. The hydration of the intermembrane space leads to an increase of membrane repeat distance with a characteristic time of 93 min. The hydration of

the hydrophilic membrane region is a 2 times faster process with a characteristic time of 44 min. The changes in the internal membrane structure take place after 1 h of hydration, as can be seen in Fig. 11. These drastic changes in the first-order structure factor are connected with structural changes in the region of the polar head groups and do not influence the membrane repeat distance. The flip-flop transformation of D-CER6 from the fully extended conformation to the one-sided conformation can explain the experimental results. This flip-flop transition of the fully extended conformation of D-CER6 is caused by the increasing membrane hydration due to swelling in water.

After 2 h of hydration, the internal membrane structure is stable in time. The last step of hydration is the swelling of the water layer between the membranes. Finally, after 8 h of hydration, the SC lipid model membrane achieves an equilibrium state with the bulk water.

The SC lipid model membrane separates into two phases at 81°C and 97% humidity from a one-phase system at 32°C. This finding demonstrates the lateral diffusion of the membrane constituents under an increase of humidity and temperature.

The SC lipid model membrane on a quartz surface offers a possibility to study the influence of other ceramides and fatty acids on the structure and properties of SC model membranes. Concerning this, it is of particular interest to apply deuterated lipids.

Acknowledgements The authors are grateful to B. Dobner for fruitful discussions and to V.L. Aksenov for support of this study. This work was supported by a grant of the Federal State of Saxony-Anhalt (project 3482A/1102L) and a grant for Support of Leading Scientific Schools. Financial assistance of the Hahn-Meitner Institute (Berlin, Germany) is gratefully acknowledged. The authors would like to thank Lipoid GmbH (Ludwigshafen, Germany) for the gift of DMPC and Cosmoferm (Delft, The Netherlands) for the gift of CER6.

References

Armen PS, Uitto OD, Feller SE (1998) Phospholipid component volumes: determination and application to bilayer structure calculations. Biophys J 75:734–744

Balagurov AM, Gordeliy VI, Yagudzhinskiy LS (1986) Investigations of sorption and desorption water kinetics in lipid membranes by neutron diffraction. Biofizika 31:1004–1010 (in Russian)

Bouwstra J, Pilgram G, Gooris G, Koerten H, Ponec M (2001) New aspects of the skin barrier organization. Skin Pharmacol Appl Skin Physiol 14(Suppl 1):52–62

Bouwstra JA, Honeywell-Nguyen PL, Gooris GS, Ponec M (2003) Sructure of skin barrier and its modulation by vesicular formations. Progress Lip Res 42:1–36

Charalambopoulou GC, Karametzanis P., Kikkinides EU, Stibos AK, Kapellopoulos NK, Papaioannou AT (2000) A study on structural and diffusion properties of porcine stratum corneum based on very small angle neutron scattering. Pharm Res 17:1085–1091

Charalambopoulou GC, Steriotis TA, Hauss T, Stefanopoulos KL, Stubos AK (2002) A Neutron diffraction study of the effect of hydration on the stratum corneum structure. J Appl Phys A 74:S1245–S1247

Feigin LA, Svergun DI (1987) Structure analysis by small-angle X-ray and neutron scattering. Plenum Publishing Corporation, New York

Franks NP (1976) Structural analysis of hydrated egg lecithin and cholesterol bilayers. J Mol Biol 100:345–358

Franks NP, Lieb WR (1979) The structure of lipid bilayers and the effects of general anaesthetics. J Mol Biol 133:469–500

Friberg SF, Osborne DW (1985) Small angle X-ray diffraction patterns of stratum corneum and a model structure for its lipids. J Dispersion Sci Technol 6:485–495

Gordeliy VI, Kiselev MA (1995) Definition of lipid membrane structural parameters from neutronographic experiments with the help of the strip function model. Biophys J 69:1424–1428

Hatfield R, Fung LWM (1995) Molecular properties of a stratum corneum model lipid system: large unilamellar vesicles. Biophys J 68:196–207

Hill JR, Wertz PW (2003) Molecular model of the intercellular lipid lamellae from epidermal stratum corneum. Biochim Biophys Acta 16:121–126

Hristova K, White SH (1998) Determination of the hydrocarbon core structure of fluid dioleoylphosphocholine (DOPC) bilayers by X-ray diffraction using specific bromination of the double-bonds: effect of hydration. Biophys J 74:2419–2433

Jager MW, Gooris GS, Dolbnya IP, Bras W, Ponec M, Bouwstra JA (2004) Novel lipid mixtures based on the synthetic ceramides reproduce the unique stratum corneum lipid organization. J Lipid Res 45:923–932

King GI, White SH (1986) Determining bilayer hydrocarbon thickness from neutron diffraction measurements using strip-function models. Biophys J 49:1047–1054

Kiselev MA, Lesieur P, Kisselev AM, Olivon M (2000) Ice formation in model biological membranes in the presence of cryoprotectors. Nucl Inst Method A 448:255–260

Kiselev MA, Zemlyanaya EV, Aswal VK (2004) SANS study of unilamellar DMPC vesicles: Fluctuation model of a lipid bilayer. Crystallogr Rep 49:s131–s136

Kucerka N, Kiselev M, Balgavy P (2004) Determination of bilayer thickness and lipid surface area in unilamellar dimyristoylphosphatidylcholine vesicles from small-angle neutron scattering curves: a comparison of evaluation methods. Eur Biophys J 33:328–334

Lemmich J, Honger T, Mortensen K, Ipsen JH, Bauer R, Mouritsen OG (1996) Solutes in small amounts provide for lipid-bilayer softness: cholesterol, short-chain lipids and bola lipids. Eur Biophys J 25:61–65

Lopez O, Cocera M, Campos L, Maza A, Coderch L, Parra JL (2000) Use of wide and small angle X-ray diffraction to study the modification in the stratum corneum induced by octyl glucoside. Colloids Surf A 162:123–130

McIntosh T (2003) Organization of skin stratum corneum extracellular lamellae: diffraction evidence for asymmetric distribution of cholesterol. Biophys J 85:1675–1681

Nagle JF, Tristram-Nagle S (2000) Structure of lipid bilayers. Biochim Biophys Acta 1469:159–195

Rand RP, Parsegion VA (1989) Hydration forces between phospholipids bilayers. Biochim Biophys Acta 988:351–376

Raudenkolb S, Wartewig S, Neubert R.H.H (2005) Polymorphism of ceramide 6. A vibrational spectroscopic and X-ray powder diffraction investigation of the diastereomers of *N*-(-hydroxy-octadecanoyl)-phytosphingosine. Chem Phys Lipids 133:89–102

Seul M, Sammon J (1990) Preparation of surfactant multilayer films on solid substrates by deposition from organic solution. Thin Solid Films 185:287–305

Tristram-Nagle S, Liu Y, Legleiter J, Nagle JF (2002) Structure of gel phase DMPC determined by X-ray diffraction. Biophys J 83:3324–3335

Wertz PW, Bergh B (1998) The physical, chemical and functional properties of lipids in the skin and other biological barriers. Chem Phys Lipids 91:85–96

Wertz PW, Abraham W, Landmann L, Downing DT (1986) Preparation of liposomes from stratum corneum lipids. J Invest Dermatol 87:582–584

White SH, Mirejovsky D, King GI (1988) Structure of lamellar lipid domains and corneocyte envelopes of murine stratum corneum. An X-ray diffraction study. Biochemistry 27:3725–3732

Wiener MC, White SH (1991) Fluid bilayer structure determination by the combined use of X-ray and neutron diffraction. Biophys J 59:162–173

Worcester DL (1976) Neutron diffraction studies of biological membranes and membrane components. Brookhaven Symp Biol 27:III37–III57

Zemlyanaya EV, Kiselev MA, Zbytovska J, Almasy L, Gutberlet T, Strunz P, Wartewig S, Klose G, Neubert RHH (2004) Study of the unilamellar vesicle structure by SANS on the basis of the SFF model. Proceedings of the Germany-JINR User Meeting "Condensed Matter Physics with Neutrons at the IBR-2 Pulsed Reactor" (June 2004, FLNP JINR, Dubna, Russia), JINR: E14-2004-148, Dubna, Russia, 83–87. http://arxiv.org/ftp/physics/papers/0410/0410244.pdf